Supplemental Figure 1
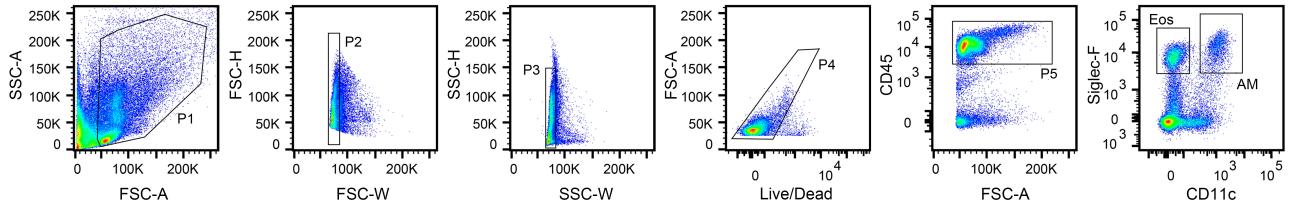
A

B

Lung CD45⁺ cells

$Pac1^{+/+}$ $Pac1^{-/-}$

5.57%   11.5%

Siglec-F-PE

CD11c-FITC

CD45⁺ cells

$p = 0.0002$

% eosinophils

C

Eosinophils

$p = 0.0040$

Number of cells

○ $Pac1^{+/+}$
○ $Pac1^{-/-}$

D

Papain Day3

$Pac1^{+/+}$ $Pac1^{-/-}$

50 µm   50 µm

E

$p = 0.0024$

Severity score
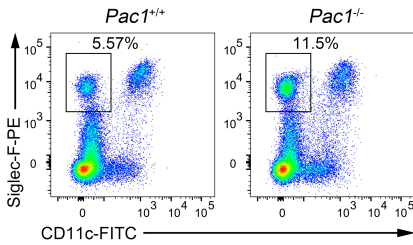
○ $Pac1^{+/+}$
○ $Pac1^{-/-}$
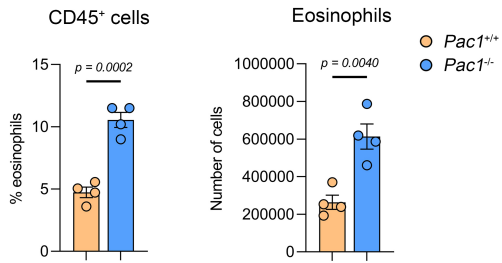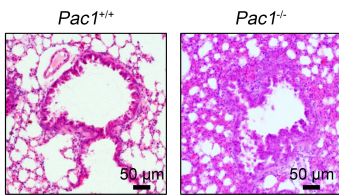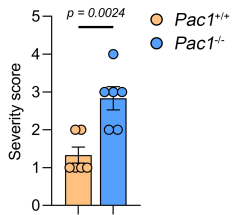
1   **Supplemental Figure 1. PAC1 constrains papain-induced allergic airway inflammation in mice**

2   **(A)** Flow cytometry plots showing the gating strategies to identify eosinophils in murine BALF or lungs.

3   **(B-C)** Frequency **(B)** and absolute number **(C)** of lung eosinophils in $Pac1^{+/+}$ ($n = 4$) and $Pac1^{-/-}$ mice ($n =$

4   4) on day 3 after papain administration, as determined by flow cytometry.

5   **(D)** Representative H&E-stained lung sections from $Pac1^{+/+}$ and $Pac1^{-/-}$ mice on day 3 after papain
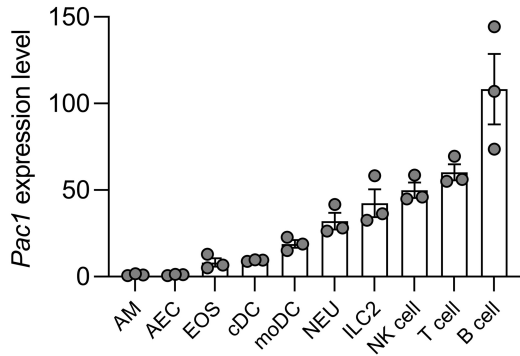
6   administration.

7   **(E)** The histological score of lungs from $Pac1^{+/+}$ ($n = 6$) and $Pac1^{-/-}$ mice ($n = 6$) on day 3 after papain

8   administration.

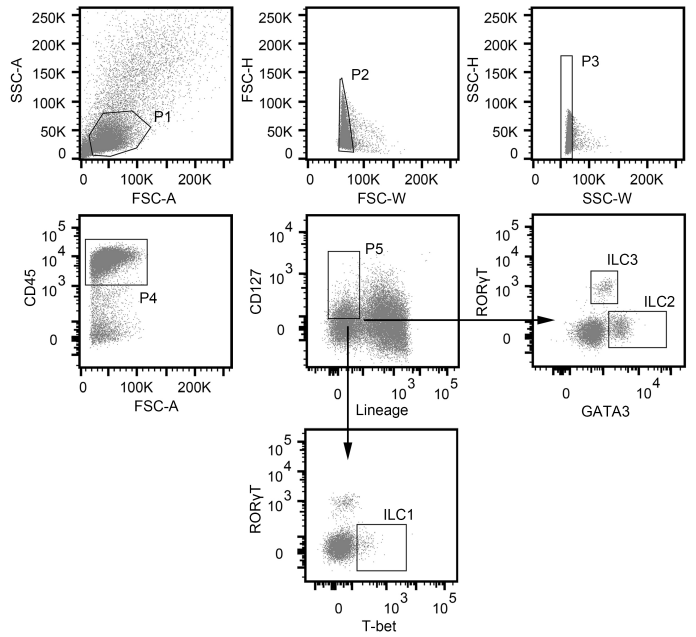9   Data are shown as the means ± SEM. Statistical significance was assessed using a two-tailed unpaired

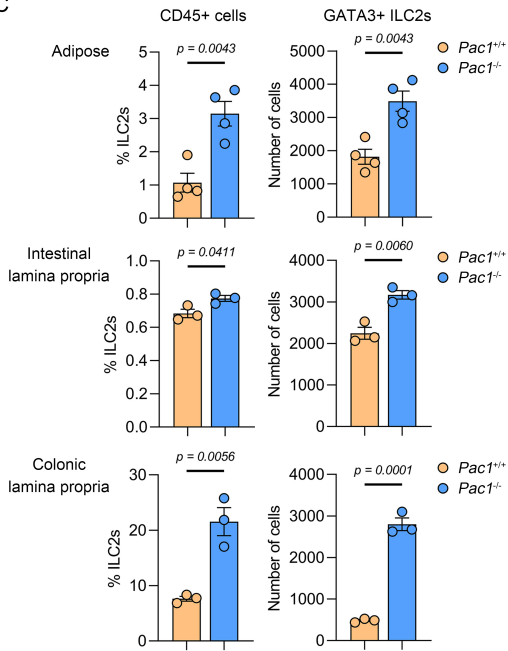10   Student's t test.

Supplemental Figure 2
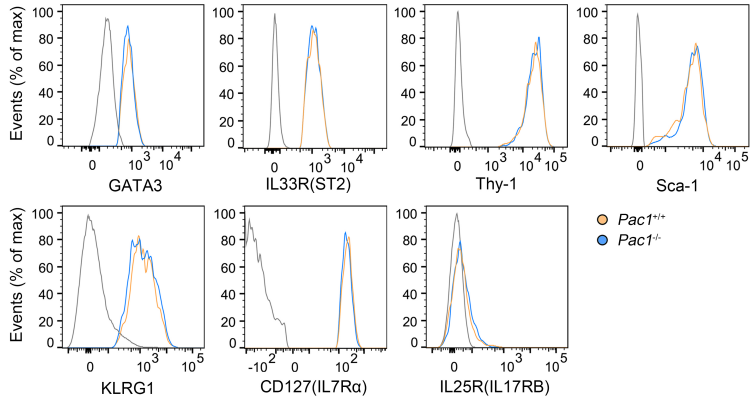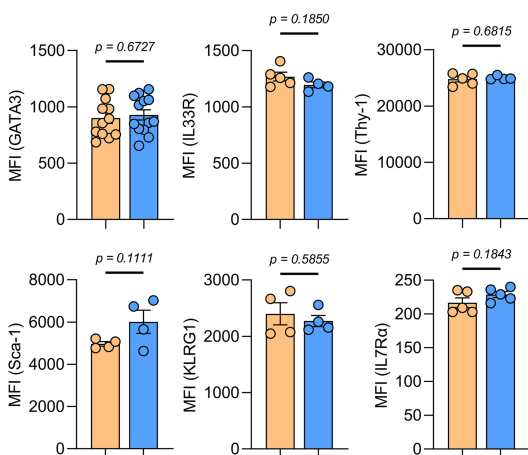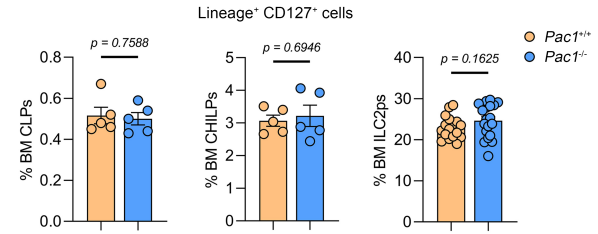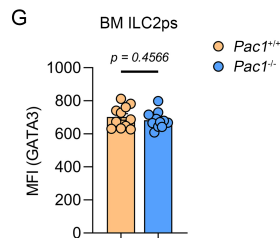
11   **Supplemental Figure 2. PAC1 is not involved in affecting the phenotype and heterogeneity of ILC2s,**

12   **and does not affect the developmental processes of ILC2s**

13   **(A)** *Pac1* expression levels in various types of cells sorted from murine lungs, as determined by qPCR. Data

14   are shown as the means ± SEM. AM, alveolar macrophages; AEC, alveolar epithelial cells; EOS,

15   eosinophils; cDC, conventional dendritic cells; moDC, monocyte-derived dendritic cells; NEU, neutrophils.

16   **(B)** Flow cytometry plots showing the gating strategies to identify T-bet$^+$ ILC1s, GATA3$^+$ ILC2s and

17   RORγT$^+$ ILC3s in murine lungs.

18   **(C)** Frequency and absolute number of GATA3$^+$ ILC2s in epididymal adipose tissue, intestinal lamina

19   propria and colonic lamina propria of *Pac1$^{+/+}$* (*n* = 3-4) and *Pac1$^{-/-}$* mice (*n* = 3-4) in their resting states, as

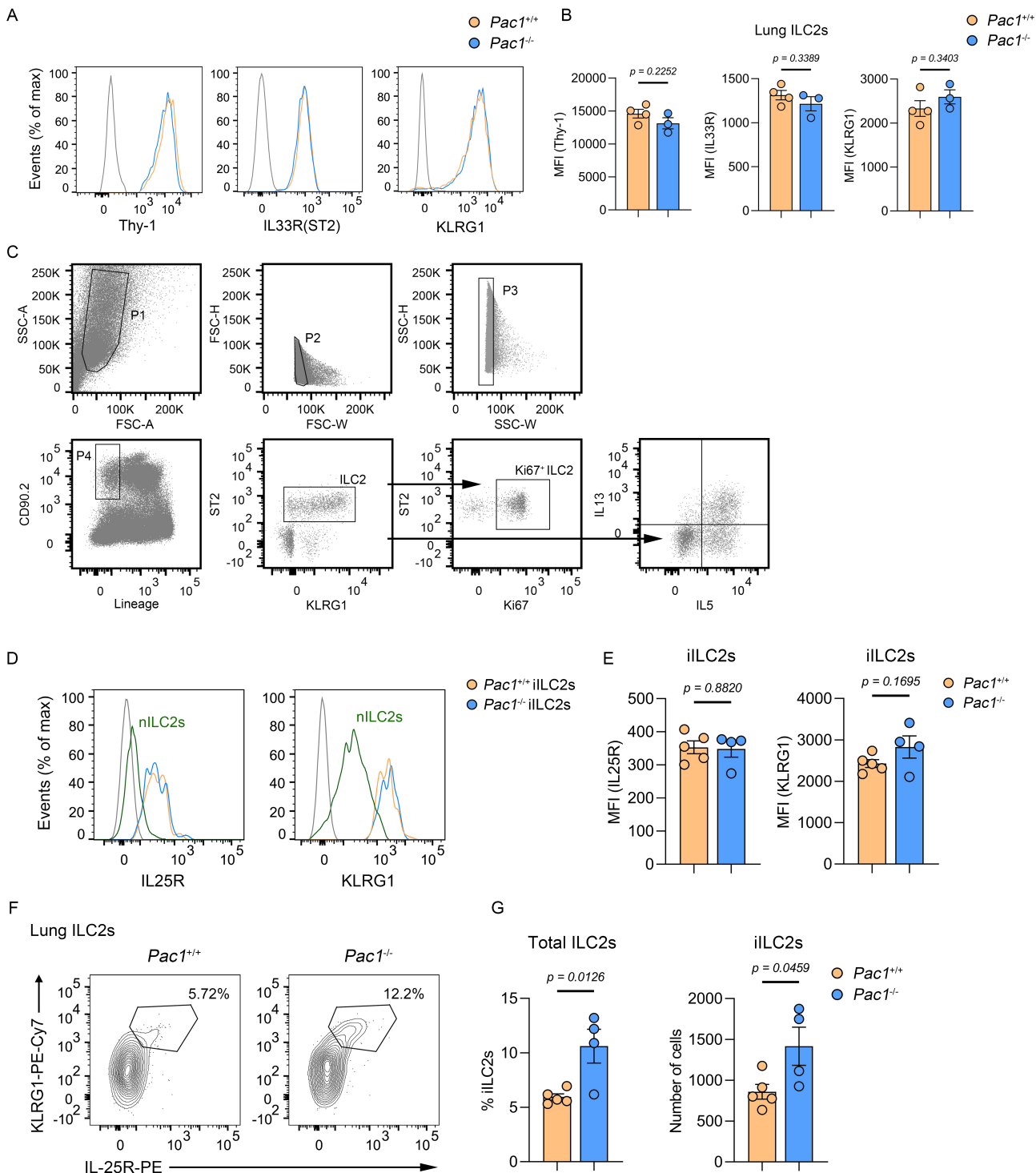20   determined by flow cytometry.

21   **(D-E)** Expression histograms **(D)** of selected ILC2 markers in *Pac1$^{+/+}$* and *Pac1$^{-/-}$* lung GATA3$^+$ ILC2s in a

22   resting states and mean fluorescence intensity (MFI) of each marker analyzed in **(E)**, as determined by flow

23   cytometry.

24   **(F)** Frequency of CLPs (*Pac1$^{+/+}$*, *n* = 5; *Pac1$^{-/-}$*, *n* = 5), CHILPs (*Pac1$^{+/+}$*, *n* = 5; *Pac1$^{-/-}$*, *n* = 5), and ILC2ps

25   (*Pac1$^{+/+}$*, *n* = 17; *Pac1$^{-/-}$*, *n* = 19) in bone marrow of *Pac1$^{+/+}$* and *Pac1$^{-/-}$* mice in their resting state, as

26   determined by flow cytometry.

27   **(G)** MFI of GATA3 in bone marrow ILC2ps (*Pac1$^{+/+}$*, *n* = 11; *Pac1$^{-/-}$*, *n* = 11) of *Pac1$^{+/+}$* and *Pac1$^{-/-}$* mice in

28   their resting state, as determined by flow cytometry.

29

30   Data are shown as the means ± SEM. Statistical significance was assessed using a two-tailed unpaired

31   Student's t test.

32

Supplemental Figure 3

A

B

Lung ILC2s

$Pac1^{+/+}$
$Pac1^{-/-}$

C

D

$Pac1^{+/+}$ iILC2s
$Pac1^{-/-}$ iILC2s

E

iILC2s
iILC2s

$Pac1^{+/+}$
$Pac1^{-/-}$

F

Lung ILC2s

$Pac1^{+/+}$ $Pac1^{-/-}$

5.72%   12.2%

G

Total ILC2s   iILC2s

$Pac1^{+/+}$
$Pac1^{-/-}$

Supplemental Figure 3. PAC1 also exhibits suppressive effects on inflammatory ILC2s

(A-B) Expression histograms (A) of selected ILC2 markers in $Pac1^{+/+}$ ($n = 4$) and $Pac1^{-/-}$ ($n = 3$) lung

GATA3$^+$ ILC2s on day 4 after IL-33 administration and mean fluorescence intensity (MFI) of each marker

analyzed in (B), as determined by flow cytometry.

(C) Flow cytometry plots showing the gating strategies to identify ILC2s, Ki67$^+$ ILC2s and IL-5$^+$ IL-13$^+$

ILC2s in murine lungs.

(D-E) Expression histograms (D) of IL-25R and KLRG1 in $Pac1^{+/+}$ ($n = 5$) and $Pac1^{-/-}$ ($n = 4$) lung

inflammatory ILC2s (iILC2s) on day 4 after IL-25 administration and mean fluorescence intensity (MFI) of

each marker analyzed in (E), as determined by flow cytometry.

(F-G) Frequency (F) and absolute number (G) of lung iILC2s in $Pac1^{+/+}$ ($n = 5$) and $Pac1^{-/-}$ mice ($n = 4$) on

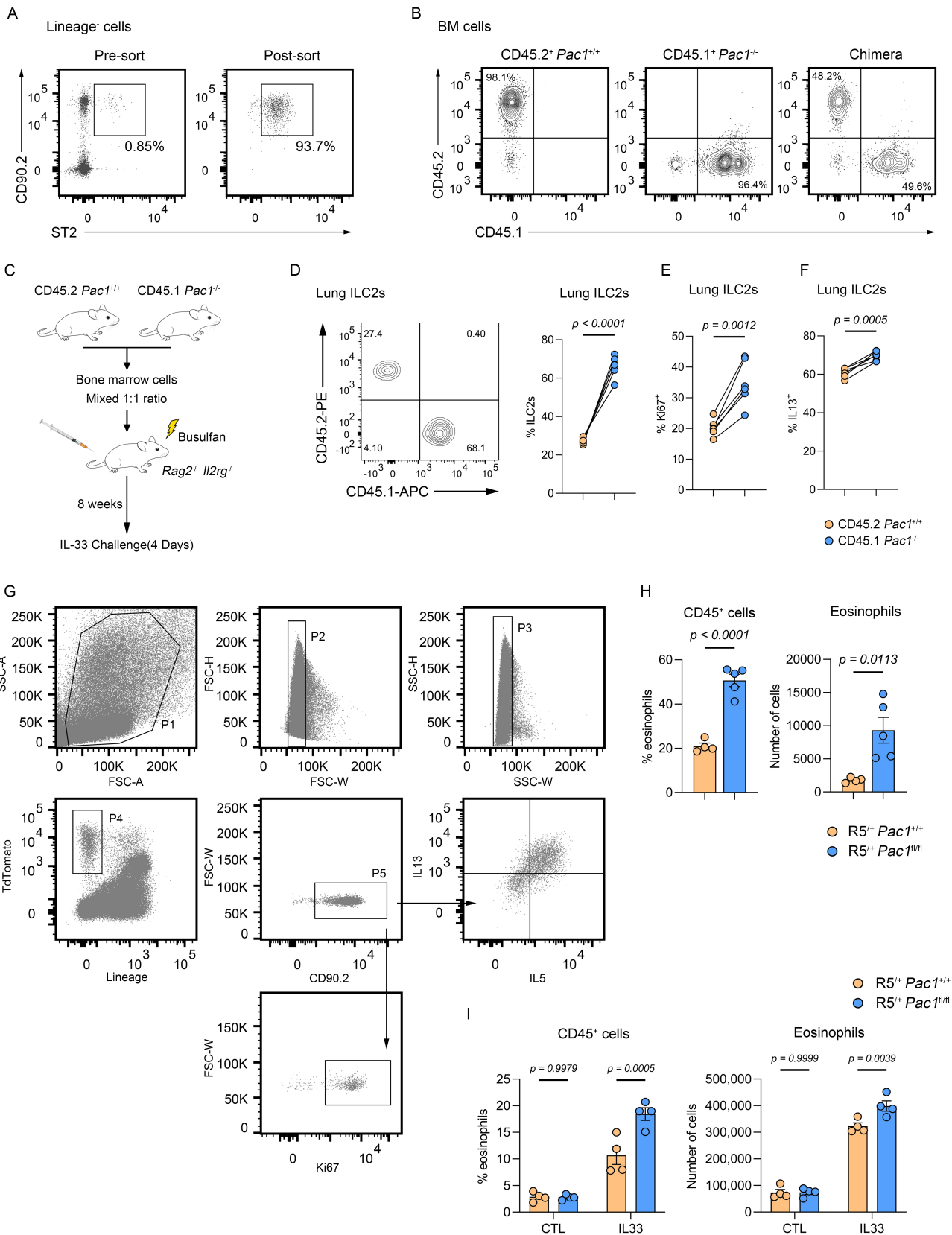day 4 after IL-25 administration, as determined by flow cytometry.

Data are shown as the means ± SEM. Statistical significance was assessed using a two-tailed unpaired

Student's t test.

Supplemental Figure 4

A
Lineage⁻ cells

B
BM cells

C

D
Lung ILC2s

E
Lung ILC2s

F
Lung ILC2s

G

H
CD45⁺ cells   Eosinophils

I
CD45⁺ cells   Eosinophils

48 **Supplemental Figure 4. PAC1 plays a cell-intrinsic inhibitory role in ILC2s**

49 **(A)** Pre-sort and post-sort purity of ILC2s from murine lungs.

50 **(B)** Frequency of CD45.1$^+$ cells and CD45.2$^+$ cells in donor CD45.2$^+$ *Pac1*$^{+/+}$ mice, donor CD45.1$^+$ *Pac1*$^{-/-}$

51 mice and recipient *Rag2*$^{-/-}$ *Il2rg*$^{-/-}$ mice in the bone marrow chimera model.

52 **(C)** Experimental protocol followed for generating mixed bone marrow chimera.

53 **(D)** Frequency of lung CD45.2$^+$ *Pac1*$^{+/+}$ ILC2s and CD45.1$^+$ *Pac1*$^{-/-}$ ILC2s in chimeric mice ($n = 6$) on day 4

54 after IL-33 administration, as determined by flow cytometry.

55 **(E)** Frequency of lung CD45.2$^+$ *Pac1*$^{+/+}$ Ki67$^+$ ILC2s and CD45.1$^+$ *Pac1*$^{-/-}$ Ki67$^+$ ILC2s in chimeric mice ($n =$

56 6) on day 4 after IL-33 administration, as determined by flow cytometry.

57 **(F)** Frequency of lung CD45.2$^+$ *Pac1*$^{+/+}$ IL-13$^+$ ILC2s and CD45.1$^+$ *Pac1*$^{-/-}$ IL-13$^+$ ILC2s in chimeric mice (n

58 $= 6$) on day 4 after IL-33 administration, as determined by flow cytometry.

59 **(G)** Flow cytometry plots showing the gating strategies to identify Ki67$^+$ ILC2s and IL-5$^+$ IL-13$^+$ ILC2s in

60 the lungs of R5$^{/+}$ mice.

61 **(H)** Frequency and absolute number of BALF eosinophils in R5$^{/+}$ *Pac1*$^{+/+}$ ($n = 4$) and R5$^{/+}$ *Pac1*$^{fl/fl}$ mice ($n =$

62 5) on day 4 after IL-33 administration, as determined by flow cytometry.

63 **(I)** Frequency and absolute number of lung eosinophils in R5$^{/+}$ *Pac1*$^{+/+}$ and R5$^{/+}$ *Pac1*$^{fl/fl}$ mice in resting state

64 (R5$^{/+}$ *Pac1*$^{+/+}$, $n = 4$; R5$^{/+}$ *Pac1*$^{fl/fl}$, $n = 4$) or on day 4 after IL-33 administration (R5$^{/+}$ *Pac1*$^{+/+}$, $n = 4$; R5$^{/+}$

65 *Pac1*$^{fl/fl}$, $n = 4$), as determined by flow cytometry.

66

67 Data are shown as the means $\pm$ SEM. Statistical significance was assessed using a two-tailed paired
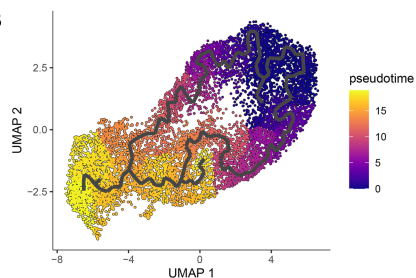
68 Student's t test (**D-F**), a two-way ANOVA followed by Holm-Sidak multiple-comparisons test (**I**) or a two-
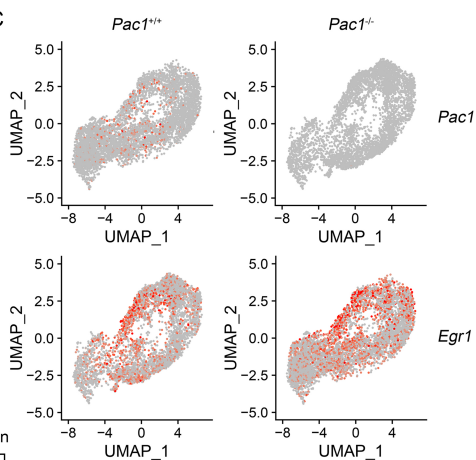
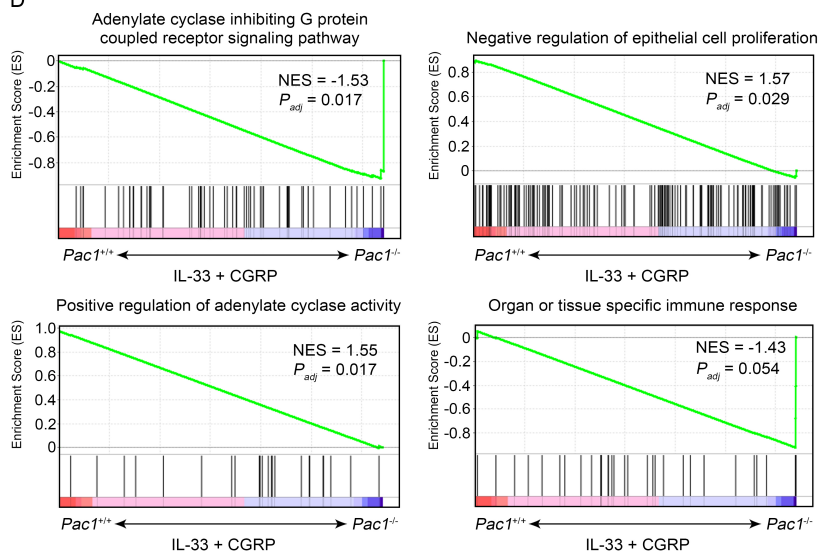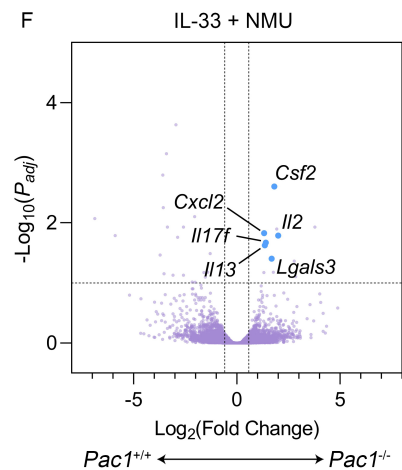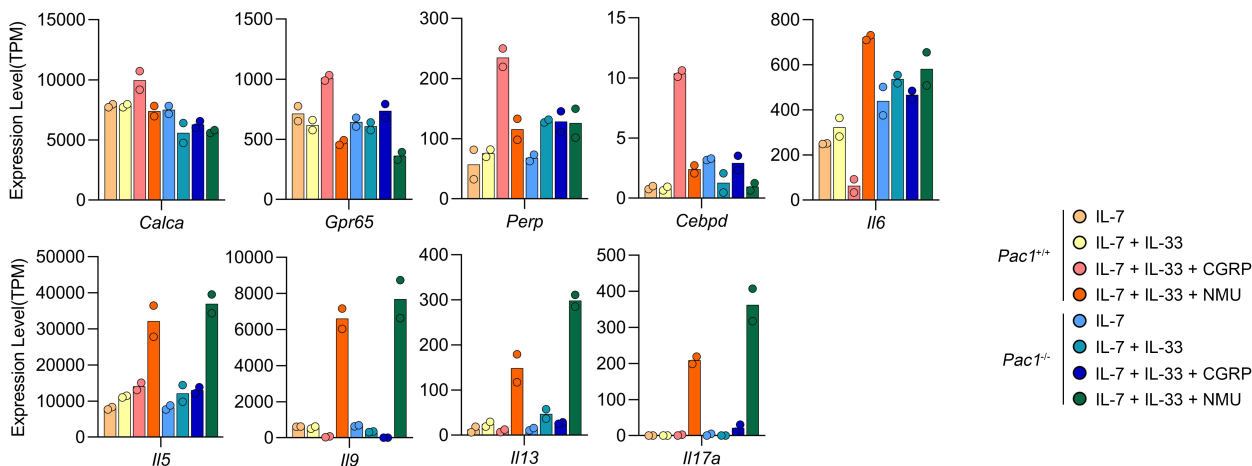69 tailed unpaired Student's t test (**H**).

70

71

72 4
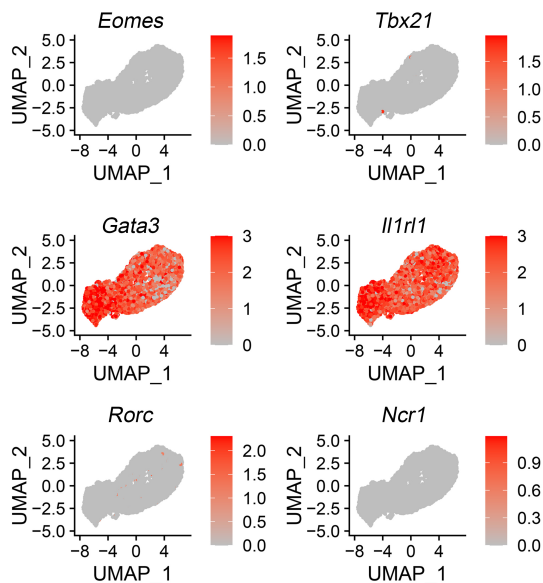
Supplemental Figure 5

73 **Supplemental Figure 5. PAC1 deficiency impairs CGRP signaling in ILC2s**

74 **(A)** Expression distribution of classic marker genes of ILC2s (*Gata3*, *Il1rl1*) or other ILC subtypes (*Eomes*,

75 *Tbx21*, *Rorc*, *Ncr1*) in sorted murine lung ILC2s.

76 **(B)** The regulation trajectory of murine lung ILC2s displayed according to a pseudotime analysis, using the

77 R package Monocle 3.

78 **(C)** Expression distribution of *Pac1* and *Egr1* in *Pac1*$^{+/+}$ and *Pac1*$^{-/-}$ lung ILC2s.

79 **(D)** GSEA plots showing representative pathways enriched in *Pac1*$^{+/+}$ and *Pac1*$^{-/-}$ murine lung ILC2s after

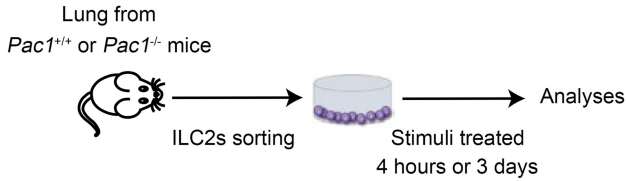80 treatment with IL-33 plus CGRP. NES, normalized enrichment score.

81 **(E)** Expression levels (transcripts per million, TPM) of representative genes in *Pac1*$^{+/+}$ and *Pac1*$^{-/-}$ murine

82 lung ILC2s under four different conditions of stimulation. Two replicates were analyzed per condition.

83 **(F)** Volcano plots of DEGs in *Pac1*$^{+/+}$ versus *Pac1*$^{-/-}$ murine lung ILC2s after treatment with IL-33 plus

84 NMU (Fold Change > 1.5; P_{adj} < 0.05). Representative DEGs are shown.
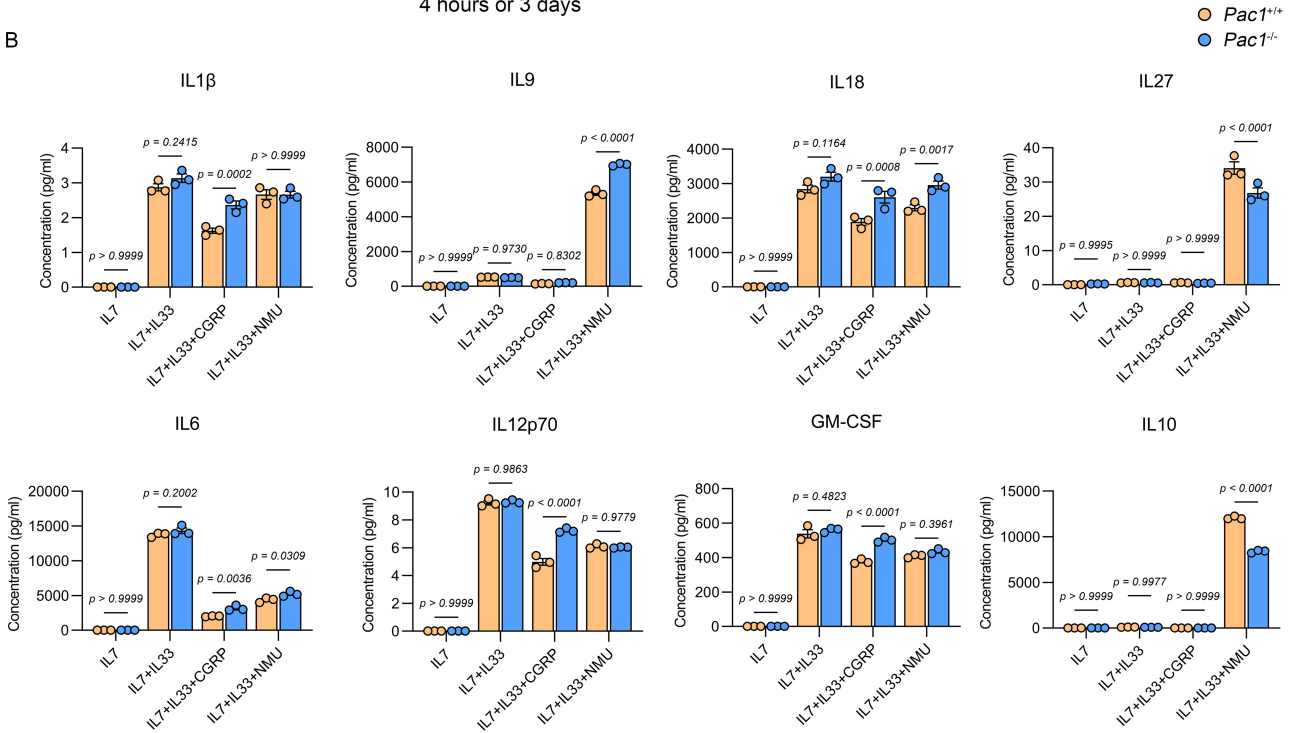
85

5

A

Lung from
Pac1^{+/+} or *Pac1*^{-/-} mice

ILC2s sorting → Stimuli treated
4 hours or 3 days → Analyses

○ *Pac1*^{+/+}
○ *Pac1*^{-/-}

B

C

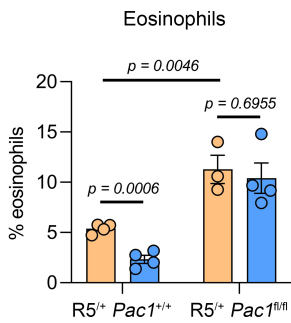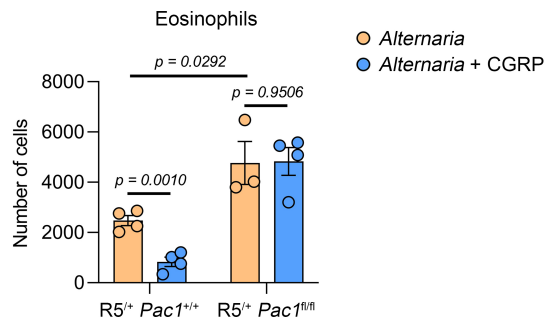Eosinophils

D

Eosinophils

○ *Alternaria*
○ *Alternaria* + CGRP

86 **Supplemental Figure 6. PAC1 promotes CGRP-mediated inhibition of ILC2 responses**

87 **(A)** Strategy for *in vitro* ILC2 stimulation.

88 **(B)** Purified *Pac1*$^{+/+}$ and *Pac1*$^{-/-}$ murine lung ILC2s were treated under different conditions of stimulation for

89 3 days, and then the concentrations of a range of cytokines in the cell supernatants were assessed by

90 Luminex liquid chip technology. Three replicates were analyzed per condition.

91 **(C-D)** Frequency **(C)** and absolute number **(D)** of BALF eosinophils in R5$^{/+}$ *Pac1*$^{+/+}$ and R5$^{/+}$ *Pac1*$^{fl/fl}$ mice

92 on day 4 after *Alternaria alternata* administration (R5$^{/+}$ *Pac1*$^{+/+}$, *n* = 4; R5$^{/+}$ *Pac1*$^{fl/fl}$, *n* = 4) or *Alternaria*

93 *alternata* plus CGRP administration (R5$^{/+}$ *Pac1*$^{+/+}$, *n* = 4; R5$^{/+}$ *Pac1*$^{fl/fl}$, *n* = 4), as determined by flow

94 cytometry.

95

96 Data are shown as the means ± SEM. Statistical significance was assessed using a two-way ANOVA

97 followed by Holm-Sidak multiple-comparisons test (**B**) or a two-tailed unpaired Student's t test (**C-D**).

98

	Forward primer (5'-3')	Reverse primer (5'-3')
mouse *Il5*	GACAAGCAATGAGACGATGAGG	CCACTCTGTACTCATCACACC
mouse *Il13*	TGGTATGGAGTGTGGACCTG	AGCAAAGTCTGATGTGAGAAAGG
mouse *Pac1*	TGCCGTGGTGCTGGATGAAA	CCTCGGGTCAGAGTTGCTATTT
mouse *Calca*	GCCTTTGAGGTCAATCTTGGA	TGGGAACAAAGTTGTCCTTCAC
mouse *Actb*	GAGACCTTCAACACCCCAGC	ATGTCACGCACGATTTCCC
human *CALCA*	CTCCATGCAGCACCATTCAG	GTGTGAAACTTGTTGAAGTCCTG
human *PAC1*	CAAGAGTATCCCTGTGGAGGAC	GAAACTGAAGTTGGGGGAGATG
human *IL13*	GAATCCCTGATCAACGTGTC	GAATCTGCAACTTCAATAGTCAGG
human *GPR65*	CGGAAGAAATATGGAAGGAAAGG	TTACACAGATATCAGCAGTTGG
human *GAPDH*	ACCCACTCCTCCACCTTTGA	ACCCACTCCTCCACCTTTGA

Supplemental Table 1. The sequences of qPCR primers used in this study